

Composition measurement of epitaxial $\text{Sc}_x\text{Ga}_{1-x}\text{N}$ films

H. C. L. Tsui¹, L. E. Goff^{1,2}, N. P. Barradas³, E. Alves^{4,5}, S. Pereira⁶, R. G. Palgrave⁷, R. J. Davies¹, H. E. Beere², I. Farrer², C. A. Nicoll², D. A. Ritchie², M. A. Moram¹

¹*Dept. Materials, Imperial College London, Exhibition Road, London SW7 2AZ, UK*

²*Dept. Physics, University of Cambridge, JJ Thomson Avenue, Cambridge CB3 0HE, UK*

³*C²TN - Centro de Ciências e Tecnologias Nucleares, Instituto Superior Técnico, Universidade de Lisboa, E.N. 10 ao km 139,7, 2695-066 Bobadela LRS, Portugal*

⁴*IPFN - Instituto de Plasmas e Fusão Nuclear, Av. Rovisco Pais, 1049-001 Lisboa, Portugal*

⁵*Laboratório de Aceleradores e Tecnologias de Radiação, Instituto Superior Técnico, Universidade de Lisboa, E.N. 10 ao km 139,7, 2695-066 Bobadela LRS, Portugal*

⁶*CICECO and Dept. Physics, Universidade de Aveiro, 3810-193 Aveiro, Portugal*

⁷*Dept. Chemistry, University College London, 20 Gordon Street, London WC1H 0AJ, UK*

Abstract

The compositions of epitaxial $\text{Sc}_x\text{Ga}_{1-x}\text{N}$ films with $0 \leq x \leq 0.26$ were measured directly using Rutherford backscattering (RBS) and X-ray photoelectron spectroscopy (XPS), and indirectly using c lattice parameter measurements from X-ray diffraction and c/a ratio measurements from electron diffraction patterns. RBS measurements were taken as a standard reference. XPS was found to underestimate the Sc content, whereas c lattice parameter and c/a ratio were not reliable for composition determination due to the unknown degree of strain relaxation in the film. However, the Sc flux used during growth was found to relate linearly with x .

Keywords: ScN, ScGaN, Rutherford backscattering, XPS, composition measurement

PACS codes: 81.05.Ea, 81.70.Jb

Introduction

III-nitride semiconductor alloys offer a wide range of band gaps from 6.2 eV to 1.9 eV¹⁻³ to widespread applications in short-wavelength optoelectronics. However, low internal quantum efficiencies remain a problem for III-nitride-based ultraviolet light emitters⁴. Challenges include the difficulty of p-type doping, alongside the relatively large lattice mismatches between layers within these devices which lead to problems with internal stresses and dislocation generation⁴. Therefore, alternative materials with wide, direct, band gaps but different lattice parameters, such as Sc-based III-nitride alloys, are of interest for improving device performance⁵.

ScN is an indirect gap semiconductor with the rock-salt structure and has been of interest recently for thermoelectric device applications⁶⁻¹¹. ScN-based interlayers are also of use as dislocation-blocking layers in the growth of epitaxial GaN films¹²⁻¹⁴. The band gaps of $\text{Sc}_x\text{Ga}_{1-x}\text{N}$ increase from 3.4 up to 4.36 eV as x increases from 0 to 0.5, while retaining the wurtzite structure¹⁵ and it is known that other physical properties, for instance the piezoelectric coefficient, are composition dependent^{16,17}. A phase transition from wurtzite to rock-salt around $x = 0.66$ is also predicted for $\text{Sc}_x\text{Ga}_{1-x}\text{N}$ ¹⁵. Therefore, accurate composition determination is crucial in order to understand the composition dependence of the properties of $\text{Sc}_x\text{Ga}_{1-x}\text{N}$ alloys and for device design and optimisation.

Rutherford backscattering spectroscopy (RBS) is an ion scattering technique used for making direct composition measurements without any standard, including compositional depth profiling for thicknesses of up to 2 μm without performing sputtering. The mass resolution of RBS is high, especially for light elements, and an accuracy of $\pm 1\%$ is commonly accepted. Another direct composition determination method is X-ray photoelectron spectroscopy (XPS), which is very surface sensitive. However, sputtering is required for depth profiling, which could affect the resulting spectrum, and the accuracy, which can be as poor as $\pm 10\%$, is not sufficient. As it is known that the lattice parameters of ternary III-nitride alloys vary as a function of composition^{18,19}, then measurements from X-ray diffraction (XRD) and electron diffraction patterns may also serve as a guide to the composition, as is standard for conventional III-nitrides²⁰. However, the lattice parameters of thin film $\text{Sc}_x\text{Ga}_{1-x}\text{N}$ may be affected by strain, which will limit the accuracy of this approach. Therefore, this study aims to evaluate and compare composition measurement methods to determine a suitable technique for use with $\text{Sc}_x\text{Ga}_{1-x}\text{N}$ thin films.

Epitaxial wurtzite-structure (0001)-oriented $\text{Sc}_x\text{Ga}_{1-x}\text{N}$ films were grown using molecular beam epitaxy (MBE) with an N_2 plasma source, under metal-rich growth conditions. A buffer layer of (0001)-oriented AlN grown by metal-organic vapour phase epitaxy (MOVPE) was deposited on the sapphire substrate. The $\text{Sc}_x\text{Ga}_{1-x}\text{N}$ film compositions were controlled by varying the Sc flux while keeping the Ga flux constant and the N_2 flow rate constant at values which produce a GaN growth rate of approximately 260 nm hr^{-1} .

Film compositions were determined using RBS as the reference. RBS measurements were performed using a beam of ^4He at 2 MeV with an incidence angle of 0° . A standard detector was placed at 140° and two pin-diode detectors located symmetrically to each other at 165° . The RBS data were analysed using the IBA DataFurnace NDF v9.6d²¹. A Thermo Scientific $\text{K}\alpha$ instrument with a monochromated Al $\text{K}\alpha$ X-ray source (1486.6 eV) was used for XPS composition analysis. Survey scans were performed by focusing X-rays at a spot size of $400\ \mu\text{m}$ with 200 eV while 50 eV was used for high resolution region scans. Sample charging was corrected by a dual beam charge compensation system and the binding energy scale was calibrated using Cu, Ag and Au. XRD for c lattice parameter determination was performed using a PANalytical MRD with a Cu $\text{K}\alpha$ source. Transmission electron microscopy (TEM) analysis was carried out using a JEOL 2100 with a high angle annular dark field (HAADF) detector operated in both dark field and scanning transmission electron microscopy (STEM) modes at 200 kV. Cross-sectional TEM samples were prepared by mechanical grinding followed by ion polishing until electron transparency was reached. The c/a ratio was measured from the electron diffraction pattern at the $\langle 01\bar{1}0 \rangle$ and $\langle \bar{2}110 \rangle$ zone axes.

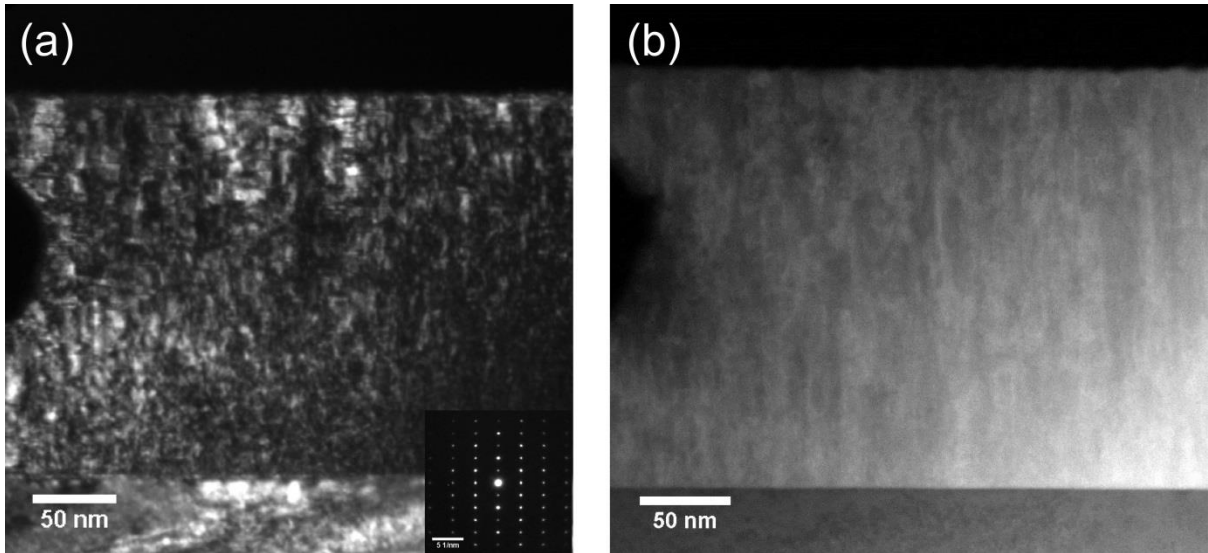


FIG. 1. (a) Cross-sectional dark field TEM image along the $\langle 11\bar{2}0 \rangle$ zone axis of $\text{Sc}_{0.258}\text{Ga}_{0.742}\text{N}$ film, insert: diffraction pattern of the $\langle 11\bar{2}0 \rangle$ zone axis; (b) Cross-sectional STEM image of the same film region in (a).

Figure 1 (a) and (b) show cross-sectional dark field TEM and STEM images of the $\text{Sc}_x\text{Ga}_{1-x}\text{N}$ films with $x = 0.26 \pm 0.01$ (the sample with the highest Sc content that still retains a phase-pure wurtzite structure). The films have a compositionally uniform microstructure without showing any evidence of phase separation. Figure 2 shows typical RBS spectra.

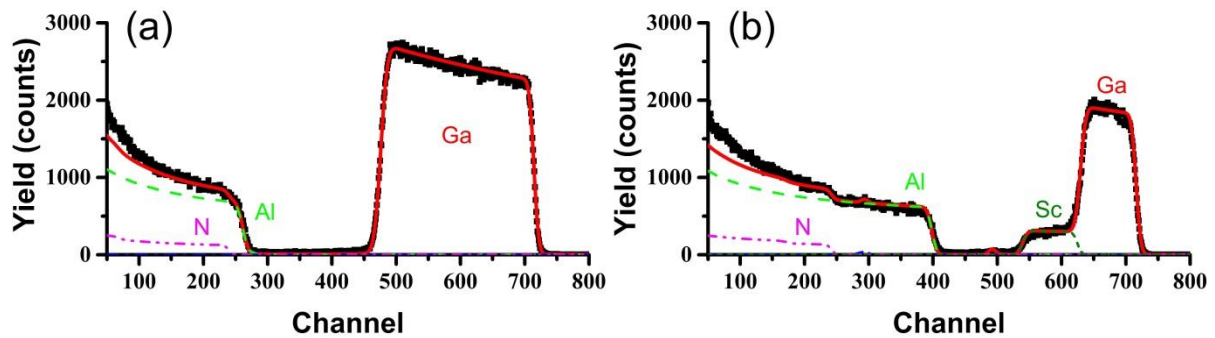


FIG. 2. RBS spectra for (a) GaN and (b) $\text{Sc}_{0.26}\text{Ga}_{0.74}\text{N}$.

Fig. 3 (a) further reveals a linear relationship between the Sc flux and x in $\text{Sc}_x\text{Ga}_{1-x}\text{N}$ as measured by RBS. For these metal-rich growth conditions, and after suitable calibration using RBS, then the Sc flux measured during growth is a very useful guide to the Sc content of the resulting film.

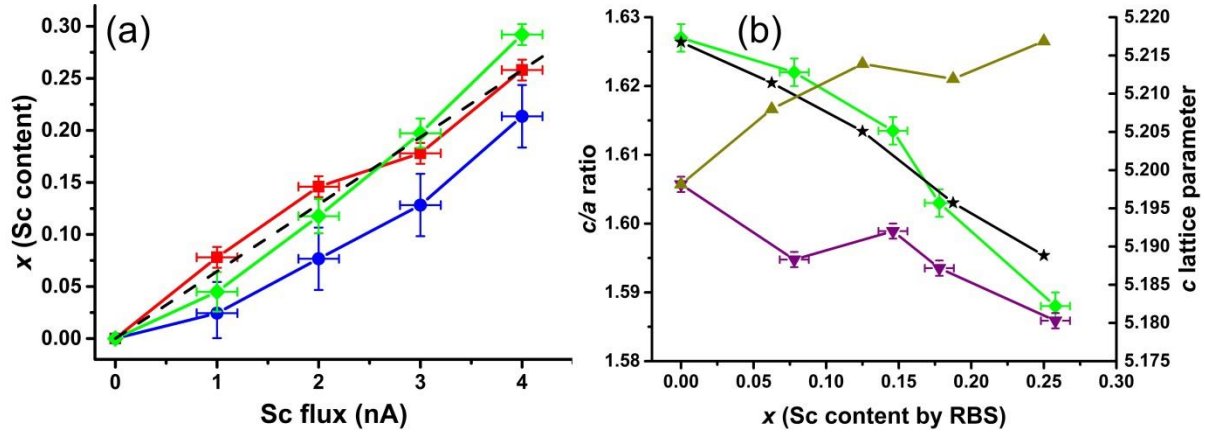


FIG. 3. (a) The relationship between the Sc flux and x in $\text{Sc}_x\text{Ga}_{1-x}\text{N}$ as measured by RBS (red squares and the dotted line indicates a linear relationship), XPS (blue circles), c/a ratio measured from electron diffraction patterns and fit to theoretical data from Ref. 15 (green diamonds); (b) c/a lattice parameter ratio: predicted (black stars, from Ref. 15) and experimental (green diamonds, from electron diffraction); c lattice parameter: predicted (dark yellow upward triangle, from Ref. 15) and experimental (purple inverted triangle, from XRD)

The compositions determined by XPS correspond to x values approximately 5-8% lower than the values obtained from RBS. XPS carried out as here with Al $K\alpha$ radiation is highly surface sensitive, with sampling depth < 10 nm. Thus the lower proportion of Sc found using XPS indicates a more Ga rich surface compared with the bulk.

Because the c and a lattice parameters of $\text{Sc}_x\text{Ga}_{1-x}\text{N}$ are expected to vary differently as a function of x , both the c/a ratio from the electron diffraction patterns and the c lattice parameter from XRD need to be compared to theoretical predictions in order to link the lattice parameter data to the composition. Both the theoretical data from Ref. 15 and the measurement show a decreasing c/a ratio as the Sc content increases, however, a significant deviation from the predicted trend is found when the Sc content is over 0.15 (Figure 3(b)). Comparing the RBS results and x estimated from the c/a ratio, it is clear that x is underestimated at low Sc content but overestimated at high Sc content (green diamond, Figure 3 (a)). This is most likely due to residual strain effects arising from differential thermal contraction of the different layers on cooling from growth temperatures (n.b. the $\text{Sc}_x\text{Ga}_{1-x}\text{N}$ film thicknesses are larger than the critical thicknesses for strain relaxation predicted from theory²² and the measured a lattice parameter of the $\text{Sc}_x\text{Ga}_{1-x}\text{N}$ films increases as x increases, consistent with strain relaxation).

In conclusion, we find that although no reliable compositional information ($0 < x < 0.26$) can be extracted from c/a ratio and c lattice parameter measurements, the Sc flux during $\text{Sc}_x\text{Ga}_{1-x}\text{N}$ growth under metal-rich conditions growth provides a reasonable guide to the resulting Sc content. It may also be possible to quantify compositions using XPS, with the aid of a calibration curve based on high-quality reference RBS data.

Acknowledgements

MAM acknowledges support through a Royal Society University Research Fellowship and through ERC Starting Grant ‘SCOPE’.

References

- ¹H. Morkoc, S. Strite, G. B. Gao, M. E. Lin, B. Sverdlov and M. Burns, *J. Appl. Phys.* **76**, 1363 (1994)
- ²A. Khan, K. Balakrishnan and T. Katona, *Nat. Photonics* **2**, 77 (2008)
- ³T. Mukai, M. Yamada and S. Nakamura, *Jpn. J. Appl. Phys.* **38**, 3976 (1999)
- ⁴M. Kneissl, T. Kolbe, C. Chua, V. Kueller, N. Lobo, J. Stellmach, A. Knauer, H. Rodriguez, S. Einfeldt, Z. Yang, N. M. Johnson and M. Weyers, *Semicond. Sci. Technol.* **26** 014036 (2011)
- ⁵M. A. Moram and S. Zhang, *J. Mater. Chem. A*, **2**, 6042 (2014)
- ⁶S. Kerdsonpanya, N. V. Nong, N. Pryds, A. Zukauskaitė, J. Jensen, J. Birch, J. Lu, L. Hultman, G. Wingqvist and P. Eklund, *Appl. Phys. Lett.* **99**, 232113 (2011)
- ⁷M. A. Moram, Z. H. Barber and C. J. Humphreys, *Thin Solid Films* **516**, 8569 (2008)
- ⁸M. A. Moram, S. V. Novikov, A. J. Kent, C. Norenberg, C. T. Foxon and C. J. Humphreys, *J. Cryst. Growth* **310**, 2746 (2008)
- ⁹J. L. Hall, M. A. Moram, A. Sanchez, S. V. Novikov, A. J. Kent, C. T. Foxon, C. J. Humphreys and R. P. Campion, *J. Cryst. Growth* **311**, 2054 (2009)
- ¹⁰H. Al-Britthen and A. R. Smith, *Appl. Phys. Lett.* **77**, 2485 (2000)
- ¹¹D. Gall, I. Petrov, L. D. Madsen, J. -E. Sundgren and J. E. Green, *J. Vac. Sci. Technol. A* **16**, 2411 (1998)
- ¹²M. A. Moram, Y. Zhang, M. J. Kappers, Z. H. Barber and C. J. Humphreys, *Appl. Phys. Lett.* **91**, 152101 (2007)
- ¹³M. A. Moram, M. J. Kappers, T. B. Joyce, P R. Chalker, Z. H. Barber and C. J. Humphreys, *J. Cryst. Growth* **308**, 302 (2007)
- ¹⁴M. A. Moram, C. F. Johnston, M. J. Kappers, C. J. Humphres, *J. Cryst. Growth* **311**, 329 (2009)
- ¹⁵S. Zhang, D. Holec, W. Y. Fu, C. J. Humphreys, and M. A. Moram, *J. Appl. Phys.* **114**, 133510 (2013)
- ¹⁶M. Akiyama, T. kamohara, K. Kano, A. Teshigahara, Y. Takeuchi and N. Kawahara, *Adv. Mater.* **21**, 593 (2009)
- ¹⁷M. Akiyama, K. Umeda, A. Honda and T. Nagase, *Appl. Phys. Lett.* **102**, 021915 (2013)
- ¹⁸H. Angerer, D. Brunner, F. Freudenberg, O. Ambacher, M. Stutzmann, R. Hopler, T. Metzger, E. Born, G. Dollinger, A. Bergmaier, S. Karsch and H. -J. Korner, *Appl. Phys. Lett.* **71**, 1504 (1997)
- ¹⁹K. P. O'Donnell, J. F. W. Mosselmans, R. W. Martin, S. Pereira and M. E. White, *J. Phys.: Condens. Matter* **13** 6977 (2001)
- ²⁰M. A. Moram and M. E. Vickers, *Rep. Prog. Phys.* **72**, 036502 (2009)
- ²¹N. P. Barradas, E. Alves, C. Jeynes and M. Tosaki, *Nucl. Instrum. Methods Phys. Res. B* **247** 381 (2006)
- ²²S. Zhang, W. Y. Fu, D. Holec, C. J. Humphreys and M. A. Moram, *J. Appl. Phys.* **114**, 243516 (2013)